Regulation of PutA−Membrane Associations by Flavin Adenine Dinucleotide Reduction†

Weimin Zhang, Yuzhen Zhou, and Donald F. Becker*

Department of Biochemistry, Redox Biology Center, University of Nebraska, Lincoln, Nebraska 68588

Received July 2, 2004; Revised Manuscript Received August 17, 2004

ABSTRACT: Proline utilization A (PutA) from *Escherichia coli* is a multifunctional flavoprotein that is both a transcriptional repressor of the proline utilization (*put*) genes and a membrane-associated enzyme which catalyzes the 4-electron oxidation of proline to glutamate. Previously, proline was shown to induce PutA−membrane binding and alter the intracellular location and function of PutA. To distinguish the roles of substrate binding and FAD reduction in the mechanism of how PutA changes from a DNA-binding protein to a membrane-bound enzyme, the kinetic parameters of PutA−membrane binding were measured under different conditions using model lipid bilayers and surface plasmon resonance (SPR). The effects of proline, FAD reduction, and proline analogues on PutA−membrane associations were determined. Oxidized PutA shows no binding to *E. coli* polar lipid vesicles. In contrast, proline and sodium dithionite induce tight binding of PutA to the lipid bilayer with indistinguishable kinetic parameters and an estimated dissociation constant (K_D) of <0.01 nM (pH 7.4) for the reduced PutA−lipid complex. Proline analogues such as L-THFA and DL-P5C also stimulate PutA binding to *E. coli* polar lipid vesicles with K_D values ranging from ∼3.6 to 34 nM (pH 7.4) for the PutA−lipid complex. The greater PutA−membrane binding affinity (>300-fold) generated by FAD reduction relative to the nonreducing ligands demonstrates that FAD reduction controls PutA−membrane associations. On the basis of SPR kinetic analysis with differently charged lipid bilayers, the driving force for PutA−membrane binding is primarily hydrophobic. In the SPR experiments membrane-bound PutA did not bind *put* control DNA, confirming that the membrane-binding and DNA-binding activities of PutA are mutually exclusive. A model for the regulation of PutA is described in which the overall translocation of PutA from the cytoplasm to the membrane is driven by FAD reduction and the subsequent energy difference (∼24 kJ/mol) between PutA−membrane and PutA−DNA binding.

The multifunctional proline utilization A (PutA) flavoprotein from *Escherichia coli* and *Salmonella typhimurium* is both a transcriptional repressor and a membrane-associated enzyme (*1*−*5*). PutA regulates the *put* regulon, which contains the genes *putA* and *putP* (Na^+/proline transporter) that are transcribed in opposite directions from the *put* control intergenic DNA (*1*, *5*−*7*). PutA represses transcription of the *put* genes by binding to specific sequences in the *put* control DNA region (*2*, *8*). The enzyme action of PutA coordinates stepwise proline dehydrogenase (PRODH)[1] and Δ^1-pyrroline-5-carboxylate dehydrogenase (P5CDH) activities, allowing bacteria to utilize proline as a sole nitrogen and energy source. The PRODH active site couples the oxidation of proline to the reduction of noncovalently bound flavin adenine dinucleotide (FAD) to form Δ^1-pyrroline-5-carboxylate (P5C) (*9*). Reduced FAD is subsequently oxidized by an electron acceptor in the membrane to regenerate oxidized FAD and complete the PRODH catalytic cycle (*3*, *10*). Next, P5C is hydrolyzed to γ-glutamic acid semialdehyde followed by a NAD-dependent oxidation to glutamate catalyzed by the P5CDH domain (*3*, *11*).

PutA has been most extensively studied from *E. coli* and *S. typhimurium*. From these bacteria, PutA is a polypeptide of 1320 amino acids with 91.3% sequence identity (*5*). PutA from *E. coli*, the subject of this study, purifies predominately as a dimer with a molecular mass of 293 kDa (*2*). The PRODH- and DNA-binding domains of PutA have been identified by structural and biochemical characterization of truncated PutA proteins (*12*−*14*). The X-ray crystal structure of a truncated form of *E. coli* PutA containing residues 1−669 (PutA669) complexed to the competitive inhibitor L-lactate was solved to 2.0 Å resolution (*13*). The crystal structure included residues 87−612 of PutA669 and revealed

† This research was supported in part by NSF Grant MCB0091664, NIH Grant GM61068, the University of Nebraska Biochemistry Department and Redox Biology Center, and the Nebraska Agricultural Research Division, Journal Series No. 14680. This publication was also made possible by NIH Grant P20 RR-017675-02 from the National Center for Research Resources. Its contents are solely the responsibility of the authors and do not necessarily represent the official views of the NIH.

* Address correspondence to this author. E-mail: dbecker3@unl.edu. Phone: 402-472-9652. Fax: 402-472-7842.

[1] Abbreviations: FAD, flavin adenine dinucleotide; *put*, proline utilization; NAD, nicotinamide adenine dinucleotide; PRODH, proline dehydrogenase; P5CDH, Δ^1-pyrroline-5-carboxylate dehydrogenase; P5C, Δ^1-pyrroline-5-carboxylate; THFA, tetrahydro-2-furoic acid; DCPIP, dichlorophenolindophenol; HEPES, *N*-(2-hydroxyethyl)piperazine-*N*′-2-ethanesulfonic acid; E_m, midpoint potential; SPR, surface plasmon resonance; SUV, small unilamellar vesicle; EDOPC, 1,2-dioleoyl-*sn*-glycero-3-ethylphosphocholine; CHAPS, 3-[(3-cholamidopropyl)dimethylammonio]-1-propanesulfonate.

10.1021/bi048596g CCC: $27.50 © 2004 American Chemical Society
Published on Web 09/25/2004

that the PRODH domain is a $\beta_8\alpha_8$ barrel comprised of residues 261−612, with the FAD bound at the C-terminal ends of the β-strands of the barrel. The DNA-binding activity of PutA involves N-terminal residues 1−47 which also appear to be important for PutA dimerization as truncation mutants (e.g., PutAΔ85) that lack these residues purify as a monomer (*14*). Primary structure analysis predicts that the P5CDH domain includes residues 650−1130 while the location of the membrane-binding domain is still unknown (*5*).

The availability of proline governs the intracellular location of PutA and whether PutA functions as a transcriptional repressor or a membrane-bound enzyme (*10*, *15*−*18*). The general model is that, in the absence of proline, PutA accumulates in the cytoplasm and represses transcription of the *put* regulon while in the presence of proline, PutA associates with the membrane. Because proline reduces FAD, the FAD redox state is thought to have a key role in regulating PutA. A redox-dependent mechanism for PutA−membrane binding was first proposed by Wood after observing enhanced steady-state kinetics of membrane association with proline and with NADH and D-lactate under anaerobic conditions (*10*). A redox mechanism was also implied from sedimentation experiments in which PutA binding to membrane vesicles and reduction of PutA-bound FAD were shown to occur at similar concentrations of proline (*16*). Surber and Maloy have also reported that PutA−membrane binding is dependent on proline reduction of FAD from studies with PutA from *S. typhimurium* using synthetic lipid vesicles and sucrose step-gradient centrifugation (*15*). Corresponding with the aforementioned studies, Brown and Wood showed that PutA undergoes a conformational change in the presence of proline that is coincident with PutA−membrane binding (*16*). Thus, proline induces a conformational change in PutA that is critical for enhancing PutA−membrane associations.

We seek to dissect the roles that proline binding and FAD reduction have in switching the intracellular location and function of PutA. Previously, controlled potentiometric proteolysis of PutA showed that FAD reduction is the chief determinant of conformational changes in PutA (*19*). However, substrate analogues that do not reduce FAD, such as L-tetrahydro-2-furoic acid (THFA), also induce a conformational change, but the resulting structure is distinct from reduced PutA (*19*). Thus, three different conformers of PutA have been identified which correspond to oxidized PutA (conformer 1), substrate analogue bound PutA (conformer 2), and reduced FAD (conformer 3). In addition to conformational studies, we have shown that substrate binding and the FAD redox state have little influence on PutA−DNA interactions. The dissociation constant of the PutA−DNA complex increases by only 2-fold in the presence of proline or upon reduction of the PutA-bound FAD (*20*). The nominal influence of FAD reduction on PutA−DNA affinity is consistent with previous studies that have shown that proline dehydrogenase activity and membrane binding are necessary for the induction of *put* gene expression (*15*, *17*, *21*, *22*).

In this report, we distinguish the impact that substrate binding and FAD reduction have on PutA−membrane associations. The effects of proline, FAD reduction, and ligand binding to the PRODH active site on the kinetics of PutA−membrane binding are explored using surface plasmon resonance (SPR) technology. SPR technology is well suited to measure the interactions of macromolecules, because association and dissociation of protein to the immobilized lipid on the surface of the sensor chip can be monitored in real time (*23*−*26*). Kinetic measurements of PutA binding to the model lipid bilayers clearly show that FAD reduction alone regulates PutA−membrane binding, proving Wood's original redox-dependent hypothesis (*10*). Our work strengthens previous studies which proposed that the disruption of the PutA−DNA complex in the cytoplasm and therefore activation of the *put* genes are due to favorable binding of reduced PutA to the membrane (*15*, *16*, *21*). Surprisingly, L-THFA and other ligands also induce membrane binding, but the membrane associations appear to be insufficient to meaningfully perturb the PutA−DNA complex. Altering the overall charge of the lipid surface has no effect on proline-reduced PutA−membrane binding, suggesting that PutA−membrane interactions are mainly hydrophobic. We believe that the described experimental system closely mimics cellular PutA−membrane interactions and provides unique insights into the regulation of PutA function.

MATERIALS AND METHODS

Chemicals. *E. coli* polar lipid extracts, phosphatidylglycerol (PG), and 1,2-dioleoyl-*sn*-glycero-3-ethylphosphocholine (EDOPC) were purchased from Avanti Polar Lipids Inc. and used without purification. 3-[(3-Cholamidopropyl)dimethylammonio]-1-propanesulfonate (CHAPS) was purchased from Novachem Biochem Corp. The L1 sensor chip and buffers for preparation of the surface were from Biacore AB (Piscataway, NJ). DL-P5C was synthesized as previously described and quantitated using *o*-aminobenzaldehyde (*27*, *28*). The 21-bp synthetic oligonucleotide 5′-TTTGCGGTTGCACCTTTCAAA-3′ and its complement were purchased from Integrated DNA Technologies. The fluorescently labeled 21-bp oligonucleotide was purchased from LI-COR, Inc. The 21-bp duplex DNA was prepared by annealing the complementary oligonucleotides in buffer (10 mM Tris, pH 8.0, 50 mM NaCl, 1 mM EDTA) by first heating at 95 °C for 5 min and then gradually cooling the sample to room temperature. The *put* intergenic DNA (419 bp) was prepared as described previously using genomic DNA from *E. coli* strain JT31 (*20*). All other buffers and chemicals were purchased from Fisher Scientific or Sigma-Aldrich Inc. All experiments used NanoPure water.

Preparation of PutA and Lipid Vesicles. PutA was overexpressed from the pET14b-PutA construct in *E. coli* strain BL21(DE3) pLysS and purified as previously described for wild-type PutA (*19*). The N-terminal hexahistidine tag was retained after purification. Size exclusion chromatography (Superdex-200 column) was then used to separate the dimeric and monomeric forms of PutA. The dimeric form was collected and used for all of the experiments. Subsequent analysis of the PutA dimer by size exclusion chromatography showed that the PutA preparation remained in the dimeric form. The concentration of PutA was determined using the BCA method (Pierce) with bovine serum albumin as the standard and spectrophotometrically using a molar extinction coefficient at 451 nm of 12700 M^{-1} cm^{-1} (*20*).

In this work small unilamellar vesicles (SUVs) of various phospholipids were used to prepare model bilayer membrane

surfaces on the L1 sensor chip. The phospholipids were received as chloroform solutions. To prepare lipid vesicles, the lipid solutions were dried by carefully flushing with N_2 gas and resuspended in 10 mM HEPES containing 150 mM NaCl at pH 7.4 (HEPES−N buffer) to a concentration of 20 mM lipid. The lipid suspensions were then subjected to 10 freeze−thaw cycles and stored frozen in liquid nitrogen. Upon thawing, the lipid suspension was diluted 100-fold with HEPES−N buffer to a final concentration of 0.2 mg/mL, except EDOPC lipid, which was prepared at a final concentration of 0.1 mg/mL. SUVs of all phospholipids were prepared by passing the lipid suspension through a 100 nm polycarbonate filter 30 times using a LiposoFast microextruder. This extrusion technique has been shown to generate unilamellar vesicles from a variety of phospholipids (*29*). EDOPC, a cationic analogue of phosphatidylcholine, also forms stable unilamellar vesicles and has been used previously to study peptide−membrane interactions (*30*, *31*). All SUVs were prepared fresh on the day of the experiment. The lipid vesicles were visualized by electron microscopy (Hitachi, Japan) and shown to have an average diameter of 100−200 nm.

Immobilization of Lipid Vesicles on the L1 Chip. PutA lipid vesicle binding experiments were performed on a Biacore 2000 instrument at 25 °C in the Genomics Core Facility in the Center for Biotechnology at the University of Nebraska. HEPES−N buffer was used as running buffer in all SPR experiments. The L1 sensor chip was washed with 20 mM CHAPS at 30 μL/min for 2 min prior to loading any lipid vesicles. Previously, Erb et al. demonstrated that lipid vesicles loaded onto a L1 sensor surface fuse together to form a lipid bilayer (*32*). For the lipid vesicles made from *E. coli* polar extracts, the sensor surface was coated with 40 μL of lipid vesicles at 5 μL/min. For PG and EDOPC lipid vesicles, the sensor surface was coated with 15 and 10 μL of lipid vesicles at 30 μL/min, respectively. After being coated with lipid vesicles, the surface was washed with 10 mM NaOH which was injected at a flow rate of 60 μL/min for 1 min to wash away multilayer and loosely immobilized vesicles on the sensor surface. The total response units (RU) for the lipid vesicle loading after NaOH washing was about 4500, 6000, and 1000 RU for the *E. coli* polar lipid extract, EDOPC, and PG, respectively. Finally, 40 μL of fatty acid free BSA (0.1 mg/mL) was injected at a flow rate 5 μL/min to block possible nonspecific protein−lipid interactions. The response observed from the BSA injection was about 1200 and 100 RU for reference and lipid vesicle coated sample flow cells, respectively. In addition to the aformentioned surface preparation, the surfaces were tested prior to each PutA-binding experiment by injecting 60 μL of BSA (0.1 mg/mL) at 30 μL/min followed by an identical injection of HEPES−N buffer. For a well-prepared reference cell, BSA and buffer injections cause response signals of <5 RU.

Surface Plasmon Resonance Analysis. PutA (13.7 μM dimer) in 10 mM HEPES buffer with 50 mM NaCl (pH 7.4) was diluted to appropriate concentrations using HEPES−N buffer. All buffers were degassed and filtered by passing through a 0.22 μm filter prior to binding experiments. The effects of L-proline, L-THFA, L-lactate, and DL-P5C on PutA−lipid binding were tested by adding the ligands to the PutA sample at a final concentration of 5 mM for 15 min prior to injection. To form the PutA−DNA complexes, *put* control DNA and 21-bp duplex DNA were added to the PutA samples at final concentrations of 300 nM and 1.8 μM, respectively, prior to injection. To test the effect of FAD reduction alone, 10 mM sodium dithionite was added to the PutA sample under anearobic conditions. Unlike proline-reduced PutA, PutA reduced with dithionite is readily reoxidized in the presence of air ($t_{1/2}$ < 0.5 min), which necessitated careful anaerobic techniques (*20*). The PutA sample was first made anaerobic by applying several cycles of argon and vacuum. Next, sodium dithionite was added to the PutA sample under a nitrogen atmosphere in a glovebox (Belle Technology). Reduced PutA samples were then placed in a vial and sealed by a rubber cap to keep PutA in the reduced state. The running buffer was also made anaerobic by applying several cycles of argon and vacuum. During the Biacore experiment, the HEPES−N running buffer was continuously flushed with nitrogen to prevent oxygenation of the buffer.

In all kinetic experiments, 120 μL of the PutA samples was injected at a flow rate of 60 μL/min. The association and dissociation phases were monitored for 120 and 300 s, respectively. Different flow rates from 20 to 80 μL/min were also used to confirm that there were no mass transfer effects during the kinetic experiments. After each protein injection, PutA and the lipid vesicles were removed from the L1 surface by applying 60 μL of CHAPS at 30 μL/min. For the simultaneous PutA−DNA and PutA−membrane binding experiments, slower flow rates from 5 to 20 μL/min were used to allow enough time for PutA to bind to the DNA or to the membrane.

The sensorgrams of PutA−lipid associations were analyzed by Biaevaluation 4.1 software. Changes in refractive index due to buffer changes were subtracted prior to kinetic analysis. Global fitting to a 1:1 Langmuir PutA−membrane binding model

$$\text{PutA} + \text{membrane} \leftrightarrow \text{PutA}-\text{membrane}$$

was used to calculate all of the kinetic and equilibrium binding constants. The association and dissociation phases of the binding reaction are described by the equations:

$$R = [k_a C/(k_a C + k_d)]R_{max}(1 - e^{-(k_a C + k_d)(t - t_0)}) + \text{RI}$$

$$R = R_0 e^{k_d(t - t_0)}$$

where R is the time-dependent response unit, k_a is the association rate constant, k_d is the dissociation rate constant, C is the concentration of analyte, R_{max} is the theoretical binding capacity, t_0 is the time at the start of the association or dissociation phase, and RI is the refractive index change of the bulk samples. The dissociation constant K_D was calculated from the equation:

$$K_D = k_d/k_a$$

DNA Binding Assays. The binding of PutA to the 21-bp oligonucleotide duplex DNA was analyzed by gel mobility shift assays using a synthetic oligonucleotide that was 5′ end-labeled with IRdye-700 (LI-COR, Inc.). The gel-shift assays were performed as previously described except that HEPES−N buffer was used to mimic the conditions of the SPR experiments (*14*). Calf thymus competitor DNA (100 μg/

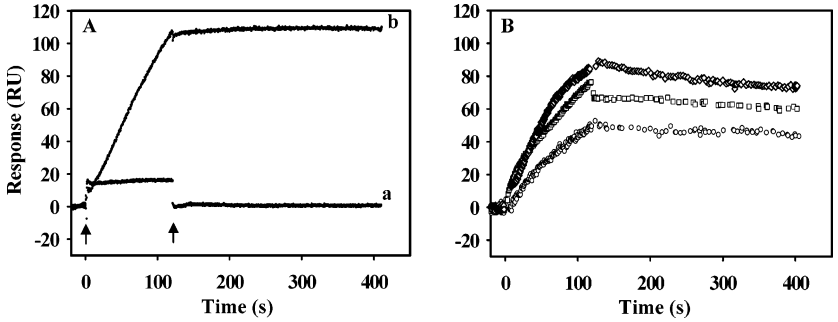

FIGURE 1: SPR sensorgrams showing proline- and ligand-induced PutA−lipid binding. Panel A: Sensorgrams of PutA (20 nM) in the oxidized state (a) and in the presence of 5 mM proline (b) binding to a lipid bilayer of *E. coli* lipid polar extracts. The arrows indicate the beginning and end of the protein sample injection. In sensorgram a, the rapid change in response units (RU) at the injection start point is due to a refractive index change of the sample, not by protein binding to the lipid bilayer. The RU returned to the initial value after the injection of the sample was complete. Panel B: Oxidized PutA (80 nM) in the presence of 5 mM L-THFA (○), 5 mM L-lactate (□), and 5 mM DL-P5C (◇) was injected at 60 μL/min for 120 s onto a L1 chip coated with *E. coli* polar lipid vesicles. The dissociation phase was observed by the flow of HEPES−N buffer at 60 μL/min for 300 s.

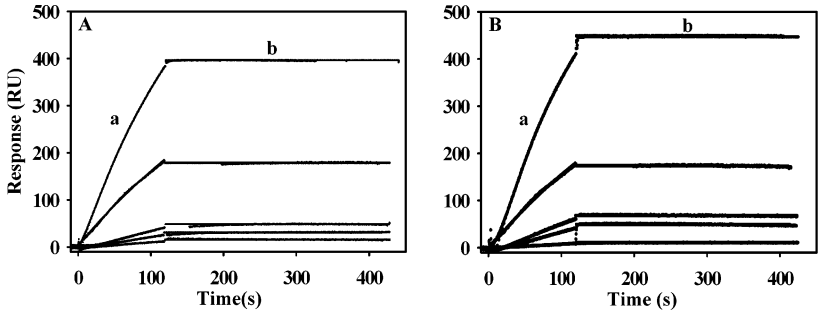

FIGURE 2: SPR sensorgrams of the association and dissociation kinetics of proline and sodium dithionite reduced PutA−lipid binding. Panel A: From bottom to top, increasing concentrations of PutA (2.5, 5, 10, 20, and 40 nM) in the presence of 5 mM proline (HEPES−N buffer, pH 7.4) were injected onto a L1 chip coated with *E. coli* polar lipid vesicles. Panel B: From bottom to top, increasing concentrations of PutA (2.5, 5, 10, 20, and 40 nM) in the presence of 10 mM sodium dithionite (HEPES−N buffer, pH 7.4) were injected onto a L1 chip coated with *E. coli* polar lipid vesicles. The association phase (a) corresponds to the injection of PutA at 60 μL/min for 120 s, and the dissociation phase (b) corresponds to the flow of HEPES−N buffer at 60 μL/min for 300 s. The data were fit by global analysis to a 1:1 Langmuir binding isotherm. Signals from the control surface have been subtracted.

mL) was added to the binding mixtures to prevent nonspecfic PutA−DNA interactions. The PutA−DNA mixtures were separated using a polyacrylamide (8%) native gel at 4 °C and visualized with a LI-COR Odyssey imager as described (*14*).

RESULTS

Proline-Dependent Membrane Binding. The phospholipid bilayer model system was first tested by assessing PutA−lipid interactions in the absence and presence of proline. Previously, proline was observed to cause about a 2-fold increase in PutA−membrane binding in sedimentation and sucrose step-gradient centrifugation experiments using inverted membrane vesicles (*15*, *16*). Sucrose step-gradient assays also showed that proline induces PutA binding to synthetic lipid vesicles (*15*). Thus, it is apparent that proline induces PutA−membrane binding and that association is generally comprised of protein−phospholipid interactions. Our initial SPR experiments with *E. coli* polar lipid vesicles confirmed these earlier results but showed a more striking proline induction of PutA−membrane binding than was previously described. Figure 1A shows that, in the absence of proline, PutA generates no repsonse, indicating that oxidized PutA does not bind to the lipid bilayer surface. After the injection of PutA is complete, the sensorgram response returns to the intial value. In stark contrast, a large response was observed for PutA in the presence of 5 mM proline (Figure 1A). Clearly, proline promotes PutA binding to the lipid vesicles. Furthermore, after injection of PutA with proline is complete and the dissociation phase begins, no significant decrease in the sensorgram signal is observed. This unique sensorgram suggests that the proline-dependent binding of PutA on the lipid bilayer is nearly irreversible or the dissociation rate is too slow to be detected by SPR.

The kinetics of PutA−lipid binding in the presence of proline were determined by measuring the senorgram response with a series of PutA concentrations ranging from 2.5 to 40 nM (Figure 2A). Because proline was kept in excess to PutA and proline-reduced PutA reacts slowly with air ($t_{1/2} \sim 125$ min), the FAD cofactor remained in the reduced state during the entire kinetic analysis (*20*). A global fit of the binding data with a 1:1 Langmuir isotherm by the Biacore evaluation software was used to estimate the kinetic constants. The association (k_a) and dissociation (k_d) rate constants were determined to be 1.4 ($\pm$0.2) $\times$ 10^5 M^{-1} s^{-1} and 10^{-6}−10^{-10} s^{-1}, respectively. An upper limit for the apparent equilibrium dissociation constant (K_D) for the PutA−lipid complex is thus <0.01 nM (Table 1). Since the limit of k_d values measured by Biacore 2000 is 10^{-6}, the proline-dependent binding of PutA to the lipid bilayer is considered to be irreversible; thus, the apparent K_D has only a relative meaning for this specific study (*33*). Attempts to release PutA from the lipid surface by injecting an artifical electron acceptor such as phenazine methosulfate (5 mM) onto the

Table 1: Kinetic and Equilibrium Binding Constants of PutA Binding to *E. coli* Polar Lipid Vesicles Determined on Biacore 2000[a]

supplement	k_a (M^{-1} s^{-1})	k_d (s^{-1})	K_D (nM)	χ^2
none	no binding			
L-proline	1.4 (±0.2) × 10^5	<10^{-6}	<0.01	0.8
L-THFA	2.3 (±0.32) × 10^4	7.8 (±0.93) × 10^{-4}	34 ± 0.5	1.4
L-lactate	2.8 (±0.13) × 10^4	3.1 (±0.22) × 10^{-4}	11 ± 0.5	0.6
DL-P5C	7.0 (±0.4) × 10^4	2.5 (±0.6) × 10^{-4}	3.6 ± 0.7	3.3
sodium dithionite	1.7 (±0.14) × 10^5	<10^{-6}	<0.01	1.1

[a] Kinetic constants were determined in HEPES−N buffer (pH 7.4) at 25 °C.

surface of the PutA−lipid complex were unsuccessful. Therefore, PutA appears to be trapped on the lipid bilayer even under oxidizing conditions.

Effects of Ligand Binding and FAD Reduction on PutA−Membrane Interactions. We next sought to distinguish the effects of ligand binding (PutA conformation 2) and FAD reduction (PutA conformation 3) on PutA−membrane binding. To mimic substrate binding, we complexed PutA with L-THFA, a nonreducing substrate analogue and a competitive inhibitor of PRODH activity in PutA (K_i = 0.2 mM) (*34*). We also tested other nonreducing compounds such as the competitive inhibitor sodium L-lactate (K_i = 1.4 mM) and the product of proline oxidation, P5C (*34*). In these experiments, PutA was incubated with 5 mM L-THFA, L-lactate, and DL-P5C for 15 min prior to injection onto the lipid bilayer surface. Figure 1B shows representative sensorgrams of PutA−lipid binding in the presence of each molecule. Each of the ligands induced PutA−membrane binding. The kinetic parameters of PutA−lipid binding in the presence of each ligand were measured as described above and are summarized in Table 1. The estimated K_D values for the PutA−lipid complex in the presence of L-THFA, L-lactate, and DL-P5C varied by 10-fold within the range of 3.6−34 nM. Thus, complexation of substrate/product analogues and inihibitors promotes analogous PutA binding to the lipid bilayer. However, marked differences in the lipid-binding properties of PutA in the presence of ligands and proline are evident. First, ligand-induced PutA−lipid binding displays reversible behavior with a noticeable dissociation phase once the injection of the PutA−ligand complex is complete. Second, the K_D values (3.6−34 nM) of the PutA−lipid complex in the presence of ligands is >300-fold higher than the upper limit of the K_D value (<0.01 nM) estimated for the PutA−lipid complex in the presence of proline (Table 1).

To study how reduction of FAD affects PutA−membrane binding, we performed SPR experiments under anearobic conditions in the presence of 10 mM sodium dithionite. Figure 2B shows that reduction of the PutA-bound FAD by sodium dithionite promotes PutA binding to the lipid bilayer surface. Interestingly, the lipid-binding behavior of PutA in the presence of sodium dithionite appears to be similar to that observed in the presence of proline (Figure 2). The kinetic parameters for PutA−lipid binding in the presence of dithionite and proline are indistinguishable (see Table 1). In addition, after injection of dithionite-reduced PutA is complete, no dissociation of PutA is observed from the lipid surface. The reoxidation of dithionite-reduced PutA with air-saturated buffer has $t_{1/2} \sim 5$ min; thus, dithionite-reduced PutA is anticipated to readily oxidize upon injecting air-saturated HEPES−N buffer. However, no significant dissociation of PutA was observed under conditions predicted to reoxidize lipid-bound PutA. The close similarities of the PutA−membrane-binding properties in the presence of proline and dithionite demonstrate that FAD reduction alone can induce PutA−lipid binding.

PutA Binding to Differently Charged Lipids. SUVs prepared from *E. coli* polar lipid extracts are negatively charged overall with about a 6:2:1 ratio (67%:23%:10%) of zwitterionic PE lipid, negatively charged PG lipid, and negatively charged cardiolipin, respectively. To study the role of phospholipid charge in PutA−lipid binding, we prepared bilayer surfaces that were either negatively charged (PG) or positively charged (EDOPC). Lipid binding of proline-reduced PutA was observed with both of the differently charged lipid bilayers. Figure 3A shows the sensorgram of proline-reduced PutA binding to positively charged EDOPC

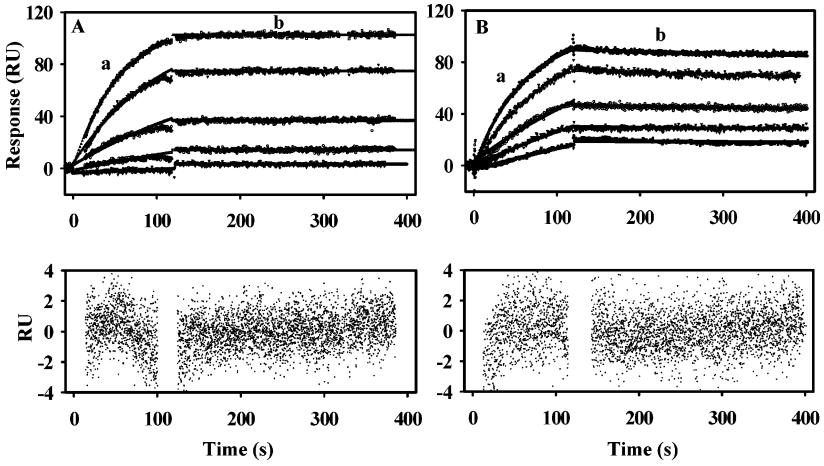

FIGURE 3: Sensorgrams of PutA binding to positively charged lipid vesicles. Panel A: Sensorgrams of proline (5 mM) reduced PutA (10, 20, 40, 80, 160 nM, bottom to top) injected onto a L1 chip coated with EDOPC lipid vesicles. Panel B: Sensorgrams of oxidized PutA (20, 40, 80, 160, 320 nM, bottom to top) injected onto a L1 chip coated with EDOPC lipid vesicles. For all sensorgrams, the association phase (a) corresponds to the injection of the PutA sample at 60 μL/min for 120 s, and the dissociation phase (b) corresponds to the flow of HEPES−N buffer at 60 μL/min for 300 s. The data were fit by global analysis to a 1:1 Langmuir binding isotherm. Signals from the control surface have been subtracted.

Table 2: Kinetic and Equilibrium Binding Constants of PutA Binding to Different Lipid Vesicles[a]

PutA and lipid surface	k_a (M^{-1} s^{-1})	k_d (s^{-1})	K_D (nM)	χ^2
proline-reduced PutA				
E. coli lipid	1.4 ($\pm$0.14) $\times$ 10^5	$<10^{-6}$	<0.01	1.6
PG lipid	4.2 ($\pm$0.43) $\times$ 10^4	$<10^{-6}$	<0.01	0.3
EDOPC lipid	1.3 ($\pm$0.04) $\times$ 10^5	$<10^{-6}$	<0.01	0.8
oxidized PutA				
E. coli lipid		no binding		
PG lipid		no binding		
EDOPC lipid	4.9 ($\pm$0.29) $\times$ 10^4	1.5 ($\pm$0.48) $\times$ 10^{-4}	3.1 $\pm$ 0.9	1.6

[a] Kinetic constants were determined in HEPES−N buffer (pH 7.4) at 25 °C.

lipids. The lipid binding of proline-reduced PutA to the negatively and positively charged lipids is characterized by similar K_D values (see Table 2) and no significant dissociation of PutA from the lipid surface. Thus, it appears that proline-reduced PutA−membrane binding is primarily hydrophobic in nature and is not significantly influenced by electrostatic interactions. Hydrophobic interactions with the membrane are also suggested by previous detergent partitioning studies that demonstrated that the relative hydrophobicity of PutA increases upon FAD reduction (*15*, *21*).

In contrast, oxidized PutA−membrane interactions are highly dependent on the overall charge of the lipids. As previously observed with lipid vesicles from *E. coli* polar extracts, oxidized PutA did not bind to a negatively charged lipid bilayer. However, oxidized PutA was observed to bind to the positively charged lipids. Figure 3B shows the sensorgram of oxidized PutA binding to the positvely charged lipid surface. The association of oxidized PutA with the lipids displays reversible binding behavior with a K_D value of 3 nM estimated for the oxidized PutA−lipid (EDOPC) complex. The kinetic parameters of oxidized PutA binding to the different lipid vesicles are summarized in Table 2. PutA is an acidic protein with an isoelectric point below pH 7.0; thus, the binding of oxidized PutA to the positively charged lipid surface appears to be influenced by electrostatic interactions, which were further explored by evaluating the influence of divalent cations.

Divalent cations such as Ca^{2+} and Mg^{2+} usually play a key role in the physiological function of protein−membrane associations and can alter the surface charge of the membrane (*35*, *36*). Because oxidized PutA interacts with positively charged lipids, we studied how Mg^{2+} may affect PutA−membrane interactions by measuring kinetic parameters of PutA−lipid binding at different Mg^{2+} concentrations. At Mg^{2+} concentrations of <0.1 mM, both oxidized PutA and proline-reduced PutA were observed to associate with lipid vesicles from *E. coli* polar extracts (data not shown). At concentrations of Mg^{2+} >1 mM, however, only proline-reduced PutA bound to the lipids. The binding of oxidized PutA to the lipids is highly influenced by Mg^{2+}, indicating a strong dependence on electrostatic interactions. At low concentrations, Mg^{2+} ions probably alter the negatively charged surface of the membrane, creating favorable electrostatic interactions between oxidized PutA and the membrane. At higher and perhaps more physiologically relevant Mg^{2+} concentrations (i.e., ~1−2 mM), the Mg^{2+} ions interfere with oxidized PutA−membrane ionic interactions. Thus, under favorable ionic conditions oxidized PutA associates with the lipids.

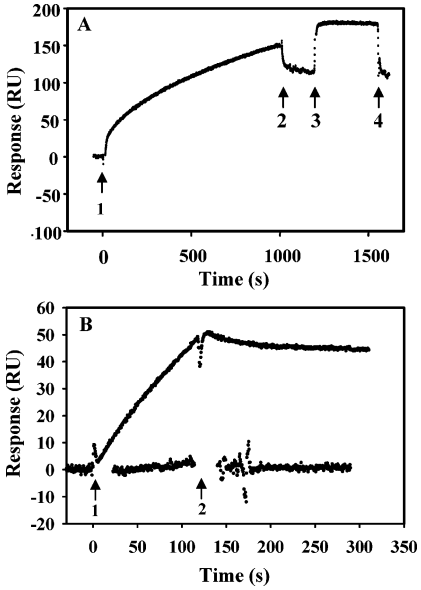

FIGURE 4: Effects of DNA binding on PutA membrane associations. Panel A: Oxidized PutA (100 nM) in the presence of sodium lactate (5 mM) was injected onto a L1 chip coated with *E. coli* polar lipid vesicles (arrows 1 and 2). The lipid-bound PutA was then washed with HEPES−N buffer at 60 μL/min for 180 s (arrows 2 and 3), followed by injection of *put* control DNA (419 bp, 20 nM) (arrows 3 and 4). The rapid change in RU at the beginning of the injection of DNA is due to the refractive index change of the DNA sample, not to PutA−DNA binding. The RU returned to the initial value after the injection of the DNA sample was complete. Panel B: Sensorgrams of the PutA (10 nM)−oligonucleotide (1.8 μM) complex (upper trace) and the PutA (10 nM)−*put* control DNA (300 nM) complex (lower trace) injected onto a L1 chip coated with *E. coli* polar lipid vesicles in the presence of 5 mM proline (arrows 1 and 2).

PutA−Membrane vs PutA−DNA Binding. PutA−DNA and PutA−membrane binding were reported to be mutually exclusive by Muro-Pastor et al. on the basis that a PutA−DNA complex was not observed in gel mobility shift assays when proline-reduced PutA was incubated simultaneously with *put* control DNA and membrane vesicles (*17*). Sedimentation experiments also showed that in the presence of proline the *put* control DNA remained in the soluble fraction and did not precipitate with the PutA−membrane complex (*17*). We sought to explore this further by testing whether PutA complexed with the lipid bilayer could bind *put* control DNA. Figure 4A shows the immoblization of PutA onto the lipid vesicles in the presence of L-lactate. Different concentrations of the *put* control DNA region (419 base pairs) from 10 to 40 nM were then injected at 5 μL/min for 15 min. No binding reponse was observed with the *put* control DNA since after the DNA injection the sensorgram returned to

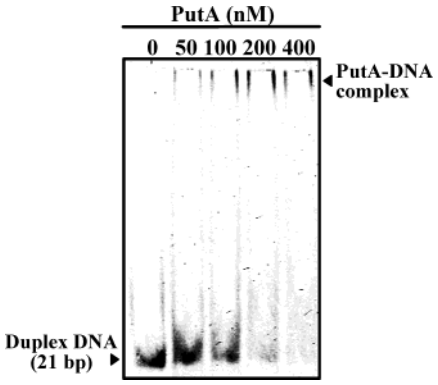

FIGURE 5: Gel mobility shift assay of the oligonucleotide binding site complexed with PutA. IRdye-700-labeled 21-bp duplex DNA (5 nM) and varying concentrations of PutA (0−400 nM dimer) were incubated in binding mixtures (HEPES−N buffer, pH 7.4) containing 100 μg/mL nonspecific calf thymus DNA at 20 °C for 20 min. The complexes were separated using a nondenaturing polyacrylamide gel (8%).

the intial value of lactate-bound PutA immobilized on the lipid surface (Figure 4A). The same result was also obtained with PutA bound to lipids in the presence of proline (data not shown). The order of binding was then reversed by first complexing PutA with DNA followed by injection of the PutA−DNA complex onto the lipid bilayer surface in the presence of proline. Figure 4B (lower trace) again shows no response in the sensorgram upon applying the proline-reduced PutA−DNA complex onto the lipid surface. Thus, the order of binding events does not influence the inability of PutA to associate concurrently with the *put* control DNA and the membrane. These results agree with the previous conclusion from gel mobility shift assays and further demonstrate that PutA−DNA and PutA−membrane binding are mutually exclusive (*17*).

The inability of PutA to bind the DNA and membrane simulatenously may indicate that recognition of a second macromolecule is not physically possible once PutA is bound to the membrane or to the *put* control DNA. PutA has been shown to have multiple DNA-binding sites and bend the *put* control DNA, suggesting the formation of a mulitmeric PutA−DNA complex (*18*). Thus, the membrane-binding domain(s) of PutA could be constrained in the PutA−DNA complex and not accessible to the membrane. Likewise, membrane-bound PutA would constrain the DNA-binding domain of PutA and prohibit DNA recognition. On the other hand, the DNA-binding and membrane-binding domains of PutA may overlap. The DNA-binding site of PutA is located in N-terminal residues 1−47 while the location of the membrane-binding region is still unknown (*14*).

To explore possible mechanisms of exclusive PutA−DNA and PutA−membrane binding, we tested whether PutA complexed with a 21-bp duplex oligonucleotide binding site (5′-TTTGCGGTTGCACCTTTCAAA-3′) could associate with the membrane. Gel mobility shift analysis in Figure 5 shows that PutA binds specifically to the 21-bp duplex DNA, forming a low-mobility complex upon increasing the concentration of PutA in the binding reactions. The PutA−DNA complex is estimated to have a K_D value of <200 nM in HEPES−N buffer. To form the PutA−DNA complex, 10 nM PutA was incubated with 1.8 μM oliognucleotide DNA for 15 min. On the basis of the upper limit for the K_D of the PutA−DNA oligonucleotide complex, >90% of the PutA is bound to the DNA. Figure 4B (upper trace) shows the sensorgram of the PutA−DNA oligonucleotide complex injected at 5 μL/min onto the lipid surface for 2 min. In contrast to the PutA−DNA complex with *put* control DNA, the PutA−DNA oligonucleotide complex associates with the lipid bilayer. However, if the order of binding is reversed, that is, when PutA is immobilized on the lipid surface prior to DNA complexation, lipid-bound PutA is not able to bind the 21-bp oligonucleotide (data not shown). Thus, the DNA- and membrane-binding sites do not overlap but instead are physically contrained when complexed to the *put* control DNA or the membrane.

DISCUSSION

FAD Reduction Activates PutA−Membrane Binding. The effects of substrate binding and FAD reduction on PutA−membrane interactions have been evaluated separately for the first time. By SPR analysis we have defined quantitatively the role of substrate binding and FAD reduction in modulating PutA−membrane interactions. The membrane binding induced by proline and dithionite reduction of PutA have the same kinetic parameters (see Table 1), demonstrating that PutA−membrane interactions are controlled by FAD redox signaling. These results confirm previous studies which proposed that FAD reduction is required for PutA−membrane associations (*10*, *15*, *16*, *21*). Nevertheless, membrane binding is also induced by complexation of PutA with nonreducing ligands such as L-THFA, L-lactate, and DL-P5C. The membrane-binding behavior of PutA in the presence of these ligands, however, is reversible and considerably weaker with K_D values >300-fold higher than that estimated for the reduced PutA−lipid complex. In previous studies by Wood, D-lactate and NADH were observed to promote PutA−membrane association under anaerobic conditions (*10*). The induction of membrane binding was explained by reduction of PutA either directly or via the respiratory chain. Our results provide an alternative explanation and show that the binding of lactate to the PRODH domain induces PutA−membrane associations. Similar to L-lactate (K_i = 1.4 mM), D-lactate (K_i = 2.1 mM) is a competitive inhibitor of PRODH activity in PutA and would also be anticipated to bind to the PRODH active site and induce PutA−membrane binding (*9*).

A distinguishing characterteristic of reduced PutA−membrane binding is that the dissociation rate is beyond the lower limits of the SPR analysis. Consequently, PutA−membrane binding in the presence of proline appears to be irreversible. Even under conditions anticipated to oxidize membrane-bound PutA, dissociation of PutA from the membrane was not observed. The data support Wood's previous suggestion that PutA−membrane associations are irreversible because under oxidizing conditions they did not detect soluble PutA protein in equilibrium with membrane vesicles harboring endogenous PutA (*10*, *16*). Irreversible PutA−membrane binding would explain how PutA remains membrane-bound during catalysis, when it is presumably cycling between redox states with high (reduced) and low (oxidized) affinity for the membrane. However, since we have no direct evidence of the FAD redox state during the SPR experiments, it is possible that when PutA is immobilized on the membrane surface, FAD is inaccessible and

remains in the reduced state regardless of the oxidizing environment.

The nature of PutA−membrane interactions appears to be largely hydrophobic on the basis of the SPR experiments with differently charged lipids. Upon FAD reduction, protein−membrane binding is likely to be promoted by interactions between hydrophobic region(s) of PutA and the lipid bilayer. Indeed, a conformational change that increases the overall hydrophobic nature of PutA has been proposed to be a mechanism by which the affinity of PutA for the membrane is enhanced upon reduction of FAD (*15*, *16*, *21*). Surber and Maloy have also shown that proline dehydrogenase activity can be reconstituted with lipid vesicles containing ubiquinone and cytochrome *bo*, indicating that PutA−membrane association involves primarily protein−lipid interactions and is not dependent on other membrane proteins (*15*). A potential membrane partner for PutA is the Na^+/proline transporter PutP. PutP has been extensively characterized, and a method for reconstituting PutP into proteoliposomes has been developed by Jung et al. (*37*−*39*). We have begun exploring the binding of proline-reduced PutA to *E. coli* polar lipid vesicles reconstituted with PutP. So far using SPR analysis, however, we have not detected any relative increase in the binding of PutA to PutP proteoliposomes, which is consistent with protein−lipid contacts being largely responsible for PutA−membrane associations (data not shown).

A useful parallel for our studies on PutA is pyruvate oxidase from *E. coli* in which reduction of the FAD cofactor also enhances membrane associations. Pyruvate oxidase catalyzes the thiamin pyrophosphate (TPP) dependent oxidation of pyruvate to acetic acid and carbon dioxide and the subsequent reduction of ubiquinone in the cytoplasmic membrane (*40*). Pyruvate or chemical reduction of the FAD cofactor in the presence of TPP exposes a lipid-binding site in the C-terminal domain of the enzyme that enables pyruvate oxidase to associate with the membrane (*41*−*45*). Because lipid binding is dependent on TPP, it is thought that changes in the FAD binding domain upon reduction are signaled to the C-terminal region of pyruvate oxidase via the TPP binding site (*45*). Communication between the FAD domain and the C-terminus is evident from spectroscopic studies, which show that the removal of the C-terminus decreases the hydrophobic character of the FAD environment (*46*). Thus, similar to that proposed for PutA, changes in the FAD redox site result in an overall conformational change that is conducive for membrane binding and converts a soluble flavoenzyme into a hydrophobic membrane-bound enzyme (*42*, *43*, *45*, *47*).

Membrane and DNA Binding Are Exclusive. PutA must switch between a transcriptional repressor and a membrane-bound enzyme to upregulate proline utilization in bacteria; thus, it seems unlikely that properly functioning PutA would bind simultaneously to the DNA and the membrane. Even so, we explored this possibility. SPR analysis with the entire *put* control DNA illustrated that PutA exclusively interacts with the DNA and the membrane. Changing the order of the binding events had no effect as PutA complexed to either the *put* control DNA or the membrane was unable to recognize an additional macromolecule in the SPR experiments (Figure 4). The exclusive macromolecular binding seems to be caused by inaccessibility of the DNA- or membrane-binding domains in the corresponding PutA−DNA and PutA−membrane complexes. Alternatively, since solution continuously flows over the lipid surface in the SPR experiments, the PutA−membrane binding reaction is not fast enough to distrupt the PutA−DNA complex equilibrium in bulk solution.

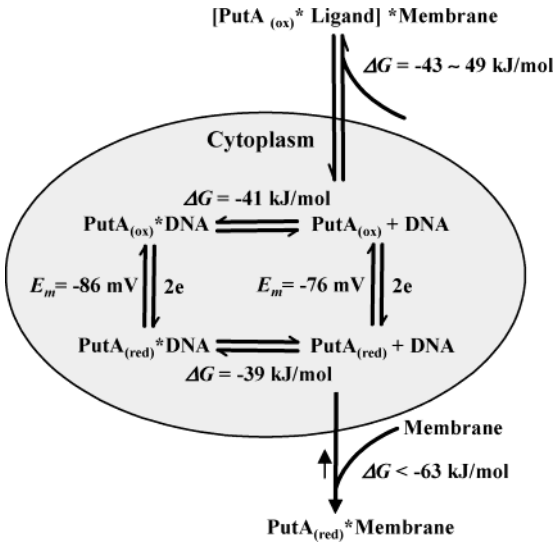

FIGURE 6: Thermodynamic model for how FAD reduction and ligand binding regulate PutA intracellular location and function (transcriptional repressor vs membrane-associated enzyme). The free energy of PutA−DNA binding and midpoint potential (E_m) values are from ref *20*, which were determined in 70 mM Tris buffer (pH 7.5) at 20 °C.

To test whether the DNA- and membrane-binding domains of PutA overlap, we repeated the experiments using a single oligonucleotide binding site from the *put* control DNA region. Again, PutA immobilized on the lipid surface did not bind the DNA, signifying that membrane binding prevents access of the oligonucleotide to the DNA-binding domain. However, reversing the order of binding events elicited the binding of the PutA−oligonucleotide complex to the lipid surface (Figure 4B). These results suggest that the DNA- and membrane-binding regions are sufficiently separated so that the binding of a 21-bp oligonucleotide to PutA does not interfere with membrane binding. We cannot exclude the possibility, however, that secondary PutA−DNA contacts occur immediately outside the 21-bp region which could interrupt PutA−membrane associations.

Regulation of PutA Intracellular Location. Until now, quantitative data describing PutA−membrane binding have not been available to provide details concerning the distribution of PutA between the DNA and the membrane. On the basis of the SPR kinetic analysis of PutA−membrane binding and previous PutA−DNA-binding studies, a model for how the intracellular location and function of PutA is regulated by proline reduction of FAD is described in Figure 6. The mechanism of PutA translocation from the cytoplasm to the membrane in Figure 6 assumes that the PutA−DNA complex does not bind to the membrane, which is supported by our work and previous observations (*17*). When PutA is in the oxidized state (conformer 1), an equilibrium exists in the cytoplasm between PutA, DNA, and the PutA−DNA complex ($K_{D,ox} \sim 45$ nM) (*20*). Upon reduction of PutA-bound FAD (conformer 3), the equilibrium of PutA, DNA, and the PutA−DNA complex ($K_{D,red} \sim 100$ nM) still exists, but now

uncomplexed reduced PutA will strongly associate with the membrane (*20*). The large energy difference (∼24 kJ/mol) between PutA−membrane and PutA−DNA binding subsequently distrupts the PutA−DNA equilibrum in the cytoplasm. As a result, the PutA−DNA complex dissociates, generating more reduced uncomplexed PutA that can bind to the membrane. Since the PutA−DNA complex cannot bind the membrane directly, PutA must first dissociate from the PutA−DNA complex before binding to the membrane. Therefore, the translocation of PutA to the membrane will depend on the dissociation rate of the PutA−DNA complex.

The surprising results with nonreducing ligands such as L-THFA and L-lactate evoke the question of what physiological impact does ligand binding have on PutA macromolecular associations? The estimated energy difference (≤8 kJ/mol) between PutA−membrane and PutA−DNA binding in the presence of ligands seems minor compared to that generated by proline. The lack of a significant driving force for PutA binding to the membrane relative to PutA−DNA binding predicts that nonreducing ligands are much less influential in regulating PutA than proline. Furthermore, PutA−membrane binding is reversible in the presence of ligands, implying that the PutA−membrane associations are in equilibrium with the PutA−DNA complex. Thus, nonreducing ligands have only a limited effect on the intracellular location and function of PutA.

From this study and previous work, it is clear that reduction of FAD bound to the PRODH active site of PutA elicits global conformational changes that direct PutA−membrane associations. Oxidized PutA is the nonmembrane-binding form (conformer 1) while reduction of FAD generates the membrane-binding form (conformer 3). Ligand-bound PutA which has a distinct conformation (conformer 2) is also capable of binding the membrane, but the association is much weaker relative to PutA conformer 3. X-ray crystallography of PutA669 and more recently PutA86−669 has revealed detailed structural information of PutA conformer 2 and the PRODH active site complexed with L-THFA, L-lactate, and acetate (*48*). Important ionic bond interactions are formed between the carboxylate group of each ligand and Arg555, Arg556, and Lys329 (*13*). Since these ligands all generate the same conformation of PutA, the carboxylate group is the minimal element required to induce PutA conformation 2. Therefore, other molecules with carboxylate groups that can bind to the PRODH active site such as pyruvic acid ($K_i = 3.3$ mM) are predicted to generate PutA conformer 2 (*9*). The mechanism for how carboxylate binding to the PRODH active site affects PutA conformation is not known, but since residues Arg555 and Arg556 are part of helix α8 of the $\beta_8\alpha_8$ barrel in the PRODH domain, helix α8 most likely is involved in transmitting signals out of the FAD active site. Work is ongoing to discover the molecular interactions that are critical for generating the different conformers of PutA and how PutA−membrane associations are controlled.

ACKNOWLEDGMENT

We thank Dr. John J. Tanner, Department of Chemistry, University of Missouri−Columbia (Columbia, MO), for sharing information concerning the crystal structure of PutA86−669 prior to publication. We thank Dr. Yuannan Xia for assistance with the SPR experiments and the Genomics Core Facility in the Center for Biotechnology for maintenance of the Biacore 2000. We also thank Dr. Jeng-Jong Shieh and Dr. James Bashkin for help in the intial stages of this SPR study and Dr. Heinrich Jung (Ludwig Maximilians University, Munich, Germany) for the generous gift of PutP proteoliposomes.

REFERENCES

1. Wood, J. M. (1981) Genetics of L-proline utilization in *Eschericia coli*, *J. Bacteriol. 146*, 895−901.
2. Brown, E., and Wood, J. M. (1992) Redesigned purification yields a fully functional PutA protein dimer from *Escherichia coli*, *J. Biol. Chem. 267*, 13086−13092.
3. Abrahamson, J. L. A., Baker, L. G., Stephenson, J. T., and Wood, J. M. (1983) Proline dehydrogenase from *Escherichia* K12, properties of the membrane-associated enzyme, *Eur. J. Biochem. 134*, 77−82.
4. Graham, S., Stephenson, J. T., and Wood, J. M. (1984) Proline dehydrogenase from *Escherichia coli* K12, reconstitution of functional membrane association, *J. Biol. Chem. 259*, 2656−2661.
5. Ling, M., Allen, S. W., and Wood, J. M. (1994) Sequence analysis identifies the proline dehydrogenase and pyrroline-5-carboxylate dehydrogenase domains of the multifunctional *Escherichia coli* PutA protein, *J. Mol. Biol. 245*, 950−956.
6. Chen, C. C., Tsuchiya, T., Yamane, Y., Wood, J. M., and Wilson, T. H. (1985) Na^+ (Li^+)-proline cotransport in *Escherichia coli*, *J. Membr. Biol. 84*, 157−164.
7. Chen, C. C., and Wilson, T. H. (1986) Solubilization and functional reconstitution of the proline transport system of *Escherichia coli*, *J. Biol. Chem. 261*, 2599−2604.
8. Nakao, T., Yamato, I., and Anraku, Y. (1987) Nucleotide sequence of *put*C, the regulatory region for the *put* regulon of *Escherichia coli* K12, *Mol. Gen. Genet. 210*, 364−368.
9. Scarpulla, R. C., and Soffer, R. L. (1978) Membrane-bound proline dehydrogenase from *Escherichia coli*, *J. Biol. Chem. 253*, 5997−6001.
10. Wood, J. (1987) Membrane association of proline dehydrogenase in *Escherichia coli* is redox dependent, *Proc. Natl. Acad. Sci. U.S.A. 84*, 373−377.
11. Menzel, R., and Roth, J. (1981) Enzymatic properties of the purified *putA* protein from *Salmonella typhimurium*, *J. Biol. Chem. 256*, 9762−9766.
12. Vinod, M. P., Bellur, P., and Becker, D. F. (2002) Electrochemical and functional characterization of the proline dehydrogenase domain of the PutA flavoprotein from *Escherichia coli*, *Biochemistry 41*, 6525−6532.
13. Lee, Y. H., Nadaraia, S., Gu, D., Becker, D. F., and Tanner, J. J. (2003) Structure of the proline dehydrogenase domain of the multifunctional PutA flavoprotein, *Nat. Struct. Biol. 10*, 109−114.
14. Gu, D., Zhou, Y., Kallhoff, V., Baban, B., Tanner, J. J., and Becker, D. F. (2004) Identification and characterization of the DNA-binding domain of the multifunctional PutA flavoenzyme, *J. Biol. Chem. 279*, 31171−31176.
15. Surber, M. W., and Maloy, S. (1999) Regulation of flavin dehydrogenase compartmentalization: Requirements for PutA-membrane association in *Salmonella typhimurium*, *Biochim. Biophys. Acta 1421*, 5−18.
16. Brown, E. D., and Wood, J. M. (1993) Conformational change and membrane association of the PutA protein are coincident with reduction of its FAD cofactor by proline, *J. Biol. Chem. 268*, 8972−8979.
17. Muro-Pastor, A. M., Ostrovsky, P., and Maloy, S. (1997) Regulation of gene expression by repressor localization: Biochemical evidence that membrane and DNA binding by the PutA protein are mutually exclusive, *J. Bacteriol. 179*, 2788−2791.
18. Ostrovsky De Spicer, P., O'Brian, K., and Maloy, S. (1991) Regulation of proline utilization in *Salmonella typhimurium*: a membrane-associated dehydrogenase binds DNA *in vitro*, *J. Bacteriol. 173*, 211−219.

19. Zhu, W., and Becker, D. F. (2003) Flavin redox state triggers conformational changes in the PutA protein from *Escherichia coli*, *Biochemistry 42*, 5469−5477.
20. Becker, D. F., and Thomas, E. A. (2001) Redox properties of the PutA protein from *Escherichia coli* and the influence of the flavin redox state on PutA-DNA interactions, *Biochemistry 40*, 4714−4722.
21. Ostrovsky De Spicer, P., and Maloy, S. (1993) PutA protein, a membrane-associated flavin dehydrogenase, acts as a redox-dependent transcriptional regulator, *Proc. Natl. Acad. Sci. U.S.A. 90*, 4295−4298.
22. Muro-Pastor, A. M., and Maloy, S. (1995) Proline dehydrogenase activity of the transcriptional repressor PutA is required for induction of the *put* operon by proline, *J. Biol. Chem. 270*, 9819−9827.
23. Stahelin, R. V., and Cho, W. (2001) Differential roles of ionic, aliphatic, and aromatic residues in membrane-protein interactions: A surface plasmon resonance study on phospholipase A2, *Biochemistry 40*, 4672−4678.
24. Bitto, E., Li, M., Tikhonov, A. M., Schlossman, M. L., and Cho, W. (2000) Mechanism of annexin I-mediated membrane aggregation, *Biochemistry 39*, 13469−13477.
25. Papo, N., and Shai, Y. (2003) Exploring peptide membrane interaction using surface plasmon resonance: Differentiation between pore formation versus membrane disruption by lytic peptides, *Biochemistry 42*, 458−466.
26. Papo, N., and Shai, Y. (2004) Effect of drastic sequence alteration and D-amino acid incorporation on the membrane binding behavior of lytic peptides, *Biochemistry 43*, 6393−6403.
27. Mezel, V. A., and Knox, W. E. (1976) Properties and analysis of a stable derivative of pyrroline-5-carboxylic acid for use in metabolic studies, *Anal. Biochem. 74*, 430−440.
28. Strecker, H. J. (1957) The interconversion of glutamic acid and proline, *J. Biol. Chem. 225*, 825−834.
29. Hope, M. J., Bally, M. B., Webb, G., and Cullis, P. R. (1985) Production of large unilamellar vesicles by a rapid extrusion procedure. Characterization of size distribution, trapped volume and ability to maintain membrane potential, *Biochim. Biophys. Acta 812*, 55−65.
30. MacDonald, R. C., Ashley, G. W., Shida, M. M., Rakhmanova, V. A., Tarahovsky, Y. S., Pantazatos, D. P., Kennedy, M. T., Pozharski, E. V., Baker, K. A., Jones, R. D., Rosenzweig, H. S., Choi, K. L., Qiu, R., and McIntosh, T. J. (1999) Physical and biological properties of cationic triesters of phosphotidylcholine, *Biophys. J. 77*, 2612−2629.
31. Lewis, R. N. A., Prenner, E. J., Kondejewski, L. H., Flach, C. R., Mednelsohn, R., Hodges, R. S., and McElhaney, R. N. (1999) Fourier transform infrared spectroscopic studies of the interaction of the antimicrobial peptide gramicidin S with lipid micelles and with lipid monolayer and bilayer membranes, *Biochemistry 38*, 15193−15203.
32. Erb, E. M., Chen, X., Allen, S., Roberts, C. J., Tendler, S. J. B., Davies, M. C., and Forsen, S. (2000) Characterization of the surfaces generated by liposome binding to the modified dextran matrix of a surface plasmon resonance sensor chip, *Anal. Biochem. 280*, 29−35.
33. Myszka, D. G. (1997) Kinetic analysis of macromolecular interactions using surface plasmon resonance biosensors, *Curr. Opin. Biotechnol. 8*, 50−57.
34. Zhu, W., Gincherman, Y., Docherty, P., Spilling, C. D., and Becker, D. F. (2002) Effects of proline analog binding on the spectroscopic and redox properties of PutA, *Arch. Biochem. Biophys. 408*, 131−136.
35. Bittova, L., Sumandea, M., and Cho, W. (1999) A structure−function study of the C2 domain of cytosolic phospholipase A2, *J. Biol. Chem. 274*, 9665−9672.
36. Ermakov, Y. A., Averbakh, A. Z., Yusipovich, A. I., and Sukharev, S. (2001) Dipole potentials indicate restructuring of the membrane interface induced by gadolinium and beryllium ions, *Biophys. J. 80*, 1851−1862.
37. Jung, H., Tebbe, S., Schmid, R., and Jung, K. (1998) Unidirectional reconstitution and characterization of purified Na^+/proline transporter of *Escherichia coli*, *Biochemistry 37*, 11083−11088.
38. Jung, H., Rubenhagen, R., Tebbe, S., Leifker, K., and Tholema, N. (1998) Topology of the Na^+/proline transporter of *Escherichia coli*, *J. Biol. Chem. 273*, 26400−26407.
39. Pirch, T., Landmeier, S., and Jung, H. (2003) Transmembrane domain II of the Na^+/proline transporter PutP of *Escherichia coli* forms part of a conformationally flexible, cytoplasmic exposed aqueous cavity within the membrane, *J. Biol. Chem. 278*, 42942−42949.
40. Koland, J. G., Miller, M. J., and Gennis, R. B. (1984) Reconstitution of the membrane-bound, ubiquinone-dependent pyruvate oxidase respiratory chain of *Escherichia coli* with the cytochrome d terminal oxidase, *Biochemistry 23*, 445−453.
41. Russell, P., Hager, L. P., and Gennis, R. B. (1977) Characterization of the proteolytic activation of pyruvate oxidase, *J. Biol. Chem. 252*, 7877−7882.
42. Schrock, H. L., and Gennis, R. B. (1977) High affinity lipid binding sites on the peripheral membrane enzyme pyruvate oxidase, *J. Biol. Chem. 252*, 5990−5995.
43. Schrock, H. L., and Gennis, R. B. (1980) The binding of a fluorescent activator 2-(N-decyl)aminonaphthalene-6-sulfonic acid to pyruvate oxidase, *Biochim. Biophys. Acta 615*, 10−18.
44. Chang, Y.-Y., and Cronan, J. E. J. (1995) Detection by site-specific disulfide cross-linking of a conformational change in binding of *Escherichia coli* pyruvate oxidase to lipid bilayers, *J. Biol. Chem. 270*, 7896−7901.
45. Chang, Y.-Y., and Cronan, J. E. J. (1997) Sulfhydryl chemistry detects three conformations of the lipid binding region of *Escherichia coli* pyruvate oxidase, *Biochemistry 36*, 11564−11573.
46. Recny, M. A., and Hager, L. P. (1983) Isolation and characterization of the protease-activated form of pyruvate oxidase. Evidence for a conformational change in the environment of the flavin prosthetic group, *J. Biol. Chem. 258*, 5189−519.
47. Russell, P., Schrock, H. L., and Gennis, R. B. (1977) Lipid activation and protease activation of pyruvate oxidase, *J. Biol. Chem. 252*, 7883−7887.
48. Zhang, M., White, T. A., Schuerman, J. P., Baban, B. A., Becker, D. F., and Tanner, J. J. (2004) Structures of the *Escherichia coli* PutA Proline Dehydrogenase Domain in Complex with Competitive Inhibitors, *Biochemistry*, in press.

BI048596G